RC22291 (W0201-024) January 3, 2002
Materials Science

IBM Research Report

Effects of Boundary Conditions and Anisotropy on Elastically Bent Silicon

S.K. Kaldor , I.C. Noyan
IBM Research Division
Thomas J. Watson Research Center
P.O. Box 218
Yorktown Heights, NY 10598

Research Division
Almaden - Austin - Beijing - Delhi - Haifa - India - T. J. Watson - Tokyo - Zurich

Effects of Boundary Conditions and Anisotropy on Elastically Bent Silicon

S.K. Kaldor and I.C. Noyan

Abstract

In four-point bending, the rollers that are used for load application impose additional constraints on the specimen that affect the anticlastic specimen curvature and cause the specimen displacement and stress profiles to deviate from the pure beam bending case. In this study, x-ray microdiffraction is used to map both the principal and anticlastic curvatures of elastically bent, rectangular (100)-type Si strips possessing width:thickness ratios of 40:1. We quantify the amount of roller constraint and show that the region over which the anticlastic specimen curvature is affected away from the roller is approximately five times the roller diameter. Consequently, for bending tests used to determine Poisson's ratio, if a region on the sample that is free from roller effects is not chosen, measurement errors as high as 46% can occur. Furthermore, we show that, due to the anisotropy of single crystal Si, this roller-constraining effect depends on crystallographic orientation and is more pronounced when the principal bending axis lies along the <100> direction as compared with the <110> direction.

Introduction

Flexural techniques, such as four-point loading, are frequently employed for accurately loading brittle materials in a variety of mechanical tests.[1-3] Depending on the sample geometry and dimensions, either the elementary beam solution or a plate solution is typically used to describe the displacement and stress profiles of a sample loaded in this configuration.[4,5] These solutions, however, do not consider the constraints imposed by the bending jig rollers used for load application. If the rollers affect either the longitudinal or transverse curvatures, errors in the

displacements or stresses predicted by an analytical solution can occur. In this paper, we compare the measured curvatures of specimens loaded in four-point bending with beam solution predictions.

Formulation

The four-point loading geometry under investigation is depicted in Figure 1 along with the Si specimen dimensions used in this study. The elementary beam solution assumes that the problem is one of cylindrical bending along the length direction and neglects the transverse effects that occur along the width direction. When a specimen is loaded in four-point bending, the upper half, or the portion of the sample lying above the neutral axis, experiences tension while the bottom half undergoes compression, and the resulting bending strain profile through the sample thickness is linear [Fig. 1(c)]. In addition to the bending strain induced along the principal bending direction (x), Poisson coupling dictates that transverse strains (y and z directions) will occur according to Eq. (1).

$$e_{yy} = e_{zz} = -n_{xy} e_{xx} \tag{1}$$

The compressive and tensile strains that occur along the transverse direction over the upper and lower half of the specimen, respectively, result in a saddle shaped deformation surface [Fig. 2]. The sample is bent to an anticlastic, rather than a cylindrical, surface where the transverse curvature along the width direction ($1/R_y$) is related to the principal curvature along the length direction ($1/R_x$), where R_x and R_y are the radii of curvature along the principal and transverse directions, respectively.[6] Rearranging Eq. (1),

$$n_{xy} = -e_{yy} / e_{xx} \tag{2}$$

and relating the maximum principal and transverse strains at the top surface to specimen curvature yields,

$$e_{xx} = -t/(2R_x) \tag{3}$$

$$e_{yy} = -t/(2R_y) \tag{4}$$

Substituting Eqs. (3) and (4) into Eq. (2),

$$n_{xy} = -R_x / R_y \tag{5}$$

Since Poisson's ratio is constant for a given material, for a given principal curvature, the specimen will be bent to a constant radius of curvature along the transverse direction. Thus, Eq. (5) provides the basis for an experimental determination of Poisson's ratio.[6,7] However, Eq. (5) assumes pure bending and does not consider the effect of the bending jig rollers on anticlastic bending. The inner rollers, which apply an upward force on the sample, should constrain anticlastic bending, at least partially. If this occurs, Eq. (5) will not hold, and the ratio of the transverse to the principal curvature will be less than the value of Poisson's ratio.

In single crystal Si, which is anisotropic, Poisson's ratio varies with sample orientation. For a cubic crystal, if a strain is applied along direction l (e.g., bending along x direction in Figure 1), the magnitude of the transverse strain that develops along orthogonal direction m will be determined by Poisson's ratio, ν_{lm}. In general, for the cubic case[8]:

$$n_{lm} = \frac{s_{12} + \left(s_{11} - s_{12} - \frac{1}{2} s_{44} \right)\left(l_1^2 m_1^2 + l_2^2 m_2^2 + l_3^2 m_3^2 \right)}{s_{11} - 2\left(s_{11} - s_{12} - \frac{1}{2} s_{44} \right)\left(l_1^2 l_2^2 + l_2^2 l_3^2 + l_1^2 l_3^2 \right)} \tag{6}$$

where s_{ij} are the elastic compliances referred to the <100> crystallographic axes, and l_i and m_i are direction cosines for l and m with respect to the <100> crystal axes. Table 1 lists values for Poisson's ratios for a Si bending sample with two different in-plane orientations. In this paper we use the notation $Si_{<hkl><uvw>}$ where <hkl> designates the crystallographic direction normal to the specimen surface (z direction), and <uvw> designates the direction parallel to the principal bending axis (y direction); the direction parallel to the transverse bending axis is uniquely defined by the cross product of these two vectors.

Table 1 Poisson's Ratio for Si strip of varied orientation (see Fig. 1)

Crystal Directions			Orientation	Poisson's Ratio
x	y	z		ν_{xy}
<100>	<010>	<001>	$Si_{<001><100>}$	0.279
<110>	<1-10>	<001>	$Si_{<001><110>}$	0.064

Table 1 illustrates that Poisson's ratio for the $Si_{<001><100>}$ case is more than four times as large as the value predicted for the $Si_{<001><110>}$ case. Since for a given principal curvature, the amount of anticlastic bending is proportional to Poisson's ratio, we expect a $Si_{<001><110>}$ sample to bend much less in the transverse direction than an equivalent $Si_{<001><100>}$ sample. Consequently, we expect the "roller effect" to be more pronounced for the $Si_{<001><100>}$ case than for the $Si_{<001><110>}$ case. In this article, we examine this effect.

Experimental

Rectangular (100) type Si single crystal specimens, 76.2 mm x 24 mm x 0.6 mm, were loaded to known displacements, $v(c_1)$, using a four-point bending jig [Fig. 1]. The bending jig, which contained two fixed rollers at x=0,a and two movable inner rollers at $x=c_1,c_2$,[9] was mounted on a diffractometer with focusing capillary optics and a motorized sample positioning stage at the X20A beamline of the National Synchrotron Light Source at Brookhaven National

Laboratory.[10] Monochromatic 8.5 KeV x-rays (wavelength = 1.459 Å) were focused to a ~10 μm diameter spot on the Si sample, and the Si 004 Bragg diffraction peak was recorded using a scintillation detector. The bending jig and Si specimen assembly were step scanned in both the x and y directions, and a rocking curve scan was performed at each increment in order to determine the amount of specimen tilt required to satisfy the Bragg condition at each position [Fig. 3]. The tilt over the specimen surface was mapped, and both the principal and transverse specimen curvatures were obtained from this data.

Figures 4(a,b) are plots of the angle required to satisfy the Bragg diffraction condition versus position along half of the specimen length for $Si_{<001><110>}$ and $Si_{<001><100>}$ samples, respectively. The angular x-ray measurements provide the specimen tilt in degrees directly, and thus these plots represent the arctangent of the first derivative of the out-of-plane displacement with respect to position along the principal bending direction, $\tan^{-1}\left(\partial v/\partial x\right)$; the sample curvature is the second derivative of the displacement with respect to position, $\partial\left(\tan^{-1}\left(\partial v/\partial x\right)\right)/\partial x$. These plots show that the curvature along the principal direction is constant (linear curves) and independent of position along the sample width, i.e. all curves overlap, and the entire sample is bent uniformly along the principal direction. The $Si_{<001><110>}$ sample was bent to $v(c_1) \approx 0.65$mm or $R_x \approx 840$mm, and the $Si_{<001><100>}$ sample was bent to $v(c_1) \approx 0.34$mm or $R_x \approx 1600$mm.

Figures 5(a,b), which correspond to $Si_{<001><110>}$ and $Si_{<001><100>}$ samples, respectively, are plots of the specimen tilt necessary to satisfy the Bragg condition versus position along the sample width. Since the displacement variation along the width direction is due to transverse bending, these curves are a measure of the amount of anticlastic bending. Near the center of the length (a/2), i.e. away from the rollers, the specimen tilt changes linearly across the sample

width, and the curvature is opposite in sign to that seen in Figures 4(a,b). Upon moving away from the center toward the inner roller, we observe a decreasing slope indicating a reduction in anticlastic bending.[11] Although the anticlastic curvature is significantly reduced at the roller, it is finite indicating that the sample bends off the roller thus resulting in a non-uniformly distributed load across the sample width. From Eq. (5), for a given material loaded to R_x, the transverse, or anticlastic, curvature should be constant along the sample length. We observe that the 6.35mm diameter, hardened steel rollers, however, limit the amount of anticlastic bending, at distances away from the roller boundary that are approximately five times the roller diameter.

This roller effect is also clearly seen in a plot of the ratio of the transverse to principal curvatures [Fig. 6(a,b)]. At the roller (c_2), the ratio of curvatures is a minimum at approximately 0.04 and 0.15 for the $Si_{<001><110>}$ and $Si_{<001><100>}$ cases respectively since the rollers limit the degree of cross sectional distortion. By reducing the amount of anticlastic bending, the rollers effectively increase the specimen's flexural rigidity. The reduction in strain along the transverse direction must be accompanied by the generation of additional constraint stresses. For the $Si_{<001><110>}$ case, the change in Poisson's ratio due to the roller effect is ~ 33% whereas for the $Si_{<001><100>}$ case, it is ~ 46%. Since Poisson's ratio determines the degree of anticlastic bending, both the stiffening effect and the magnitude of the constraint stresses will be greater for the $Si_{<001><100>}$ case than the $Si_{<001><110>}$ case.

At the length center (a/2), for both the $Si_{<001><110>}$ and $Si_{<001><100>}$ samples, this ratio attains the correct value of Poisson's ratio, 0.06 and 0.279 respectively, within experimental error.[12] This observation of unhindered anticlastic bending at the sample center illustrates two points. First, a minimum distance between the inner rollers is required in order to create a region along the sample length that is free of additional constraints imposed by the roller. This distance,

whose dependence on sample dimensions is under investigation,[13] should be considered during bending jig design. Secondly, unhindered anticlastic bending implies beam, rather than plate, behavior for the sample under investigation (b:t = 40). Until now, we have tacitly assumed that the Si strips under investigation behave as beams; this requires some justification. The width-to-thickness ratio, which is typically referred to, is not a sufficient criterion for differentiating between a beam and a plate in this case.[14] Rather, a parameter proposed by Searle[6] involving the specimen width, thickness, and longitudinal bending radius, which we term the Searle parameter (β), should be used to determine whether plane strain (plate or wide beam) or plane stress (beam) conditions are valid:[15,16]

$$b = \frac{b^2}{R_x t} \tag{7}$$

An extension of this work by Ashwell[17] showed that for $\beta < 5$, anticlastic curvature is unhindered, and the sample behaves as a beam, whereas, for $\beta > 60$, anticlastic curvature is neutralized over the majority of the sample width, and the sample behaves as a plate with increased stiffness. For the samples tested in this study ($\beta = 1.2$ and $\beta = 0.6$), we can attribute reductions in the degree of anticlastic bending solely to the roller effect.

For comparative purposes, we checked the ASTM Standard Test Methods for Strength of Glass by Flexure (Determination of Modulus of Rupture), which describes two tests (A and B).[18] In standard C158-95, Test Method A calls for samples that are approximately 250 mm in length and a spacing between the loading edges of 100 mm. While the large spacing between the inner loads will eliminate boundary effects at the specimen center, such large dimensions may not be attainable with single crystal semiconductor specimens that are cut from wafers of fixed diameters (100-300 mm). In Test Method B, two suggestions ($2 <$ b:t < 10 and $b > 9.5$ mm) for

rectangular specimens will, for most realistic cases, ensure a beam geometry. However, the recommended spacing between the inner rollers of 19 mm in this test case is not large enough to create a region on a 24 mm wide sample free from boundary (roller) effects. Furthermore, in these test methods, the maximum applied bending radius is not specified. Even when ASTM sample guidelines are followed, both the maximum bending radius and the Searle parameter should be reported.

Conclusions

We have quantified the effect of rollers on the principal and anticlastic curvatures of Si samples elastically loaded in four-point bending. The reduction in anticlastic bending caused by the rollers may lead to errors in experiments that employ this technique to apply a constant stress to a sample. Furthermore, for bending tests aimed at determining Poisson's ratio, a region on the beam sample that is free from roller effects must be chosen to ensure that Eq. (5) holds. The presence of some transverse bending at the rollers indicates that, for a beam sample, the roller is not in contact with the specimen over its entire width. Planar analytical solutions tacitly ignore this point, but, in three-dimensional finite element models, this boundary condition should be modified to account for a non-uniformly distributed load across the sample width. It should be noted that the roller effect will be present in three-point bending as well. Due to the central location of the roller in this test, this effect will be a maximum at the sample center, or the region of maximum stress that is typically chosen for measurements.

Acknowledgments

The authors thank Dr. James M.E. Harper of IBM Research and Dr. P.C. Wang of IBM Microelectronics for valuable feedback and discussions. The help of Mr.David DiMilia with

specimen dicing is also acknowledged. The work at the National Synchrotron Light Source, Brookhaven National Laboratory was supported by DOE Contract No. DE-AC02-76CH00016.

References

1. Hertzberg, R.W, Deformation and Fracture Mechanics of Engineering Materials, Wiley, New York, 42-45 (1996).

2. Klingbeil, N.W. and Beuth, J.L., "Interfacial Fracture Testing of Deposited Metal Layers Under Four-Point Bending," Engineering Fracture Mechanics, 56 (1), 113-126 (1997).

3. Scardi, P., Dong, Y.H., Setti, S., and Fontanari, V., "A 4-Point Bending Device for In Situ Measurement of Elastic Properties of Polycrystalline Materials by X-ray Diffraction," Proc. Of the Sixth Intl. Conf. On Residual Stress, Oxford, 1, 67-73 (2000).

4. Popov, E.P., Engineering Mechanics of Solids, Prentice-Hall, Englewood Cliffs, NJ, 280-311 (1990).

5. Reddy, J.N., Theory and Analysis of Elastic Plates, Taylor & Francis, Philadelphia, Ch.4 (1999).

6. Searle, G.F.C., Experimental Elasticity, Cambridge UP, 38-58 (1920).

7. Reismann, H., Elastic Plates: Theory and Application, Wiley, New York, 75-76 (1988).

8. Brantley, W.A., "Calculated Elastic Constants for Stress Problems Associated with Semiconductor Devices," J. Appl. Phys., 44 (1), 534-535 (1973).

9. The rollers were kept well lubricated to minimize frictional effects between the roller and sample as well as the roller and bending jig.

10. Noyan, I.C., Kaldor, S.K., Wang, P.-C., and Jordan-Sweet, J.L., “A Cost-Effective Method for Minimzing the Sphere-of-Confusion Error for X-ray Microdiffractometers,” Rev. Sci. Instr., 70 (2), 1300-1304 (1999).

11. It should be noted that there is no corresponding variation of these curves with the principal curvature scans. Due to the fixed roller positions, the principal curvature is determined by geometrical considerations only and is not impacted by transverse bending effects. Thus, in certain cases, a 3-D model may be necessary to accurately describe a sample’s bending response.

12. The overall error reported was obtained by propagating the standard errors associated with the linear fits to the x-ray data through Eq. (5) for both the principal and transverse curvatures.

13. For these tests (width = 24mm, roller diameter = 6.35mm), roller effects become negligible at a distance away from the roller of five times the roller diameter. For cases where the sample width is smaller than the roller diameter, the region affected by the rollers may be related to the specimen width. This point is under investigation.

14. Kaldor, S.K. and I.C. Noyan, “Deflection and X-ray Studies of Samples Loaded in Bending,” Proceedings of the SEM IX International Congress on Experimental Mechanics, Orlando, FL, 808-811 (June 2000).

15. Kaldor, S.K. and Noyan, I.C., “Differentiating between elastically-bent rectangular beams and plates,” To be published in Applied Physics Letters.

16. Kaldor, S.K., “X-ray Microbeam Studies of Anticlastic Curvature in Elastically-Bent (100)-type Silicon Beams and Plates,” Ph.D. Thesis, Columbia University (2002).

17. Ashwell, D.G., “The Pure Bending of Rectangular Plates,” Engineering, July 21, 1950, 51-52 and July 28, 1950, 76-78.

18. “Standard Test Methods for Strength of Glass by Flexure (Determination of Modulus of Rupture)," ASTM Standard C158-95, American Society for Testing and Materials, Philadelphia (1995).

Figure 1. (a) Si specimen geometry and dimensions, (b) 2-D schematic of bent sample (displacement applied at c_1 and c_2 rollers), and (c) bending strain variation, ε_{xx}, with sample thickness, z.

Figure 2. (a) The rectangular specimen is bent with a radius of curvature, R_x, along the principal bending direction, x. Poisson coupling causes the sample to bend along the transverse (y) direction with a radius of curvature, R_y, equal to R_x/ν thus resulting in an anticlastic, or saddle-shaped, surface. (b) The anticlastic-bending strain variation, ε_{yy}, with specimen thickness, z.

Figure 3. Schematic of the x-ray diffraction measurement. Given the correct Bragg angle (θ) between the sample surface and incident x-ray beam, x-rays will diffract from the Si (001) planes, i.e. those planes normal to the Si surface in a (100)-type crystal. For the unbent, flat single crystal in (a), the specimen tilt, ψ, necessary to satisfy the Bragg diffraction angle, θ, is independent of sample position. For the sample bent to a constant principal radius in (b), ψ necessary to satisfy θ will change with position along both the principal and transverse directions. The sample rotation required to satisfy the Bragg diffraction in (b) gives the specimen curvature.

Figure 4. The sample tilt required to satisfy the Bragg condition for (004) diffraction from a Si (001) crystal as a function of position along the sample length at several distinct positions along the sample's width. The straight, overlapping lines indicate that the principal curvature is constant between the two inner rollers and does not vary with position along the sample width. In (a) the principal bending axis is parallel to the <110> direction ($Si_{<001><110>}$) whereas in (b) it is parallel to the <100> ($Si_{<001><100>}$) direction.

Figure 5. The sample tilt required to satisfy the Bragg condition for (004) diffraction from a Si (001) crystal as a function of position along the sample width at several distinct positions along

the sample's length. Unlike the principal curvature, these curves, whose slopes are a measure of anticlastic bending, vary with position along the sample length. In (a) the principal bending axis is parallel to the <110> direction ($Si_{<001><110>}$) whereas in (b) it is parallel to the <100> direction ($Si_{<001><100>}$).

Figure 6. Variation of the ratio of transverse to principal curvatures with position along the sample length for (a) a $Si_{<001><110>}$ sample and (b) a $Si_{<001><100>}$ sample. The presence of rollers in this four-point loading configuration affects anticlastic bending.

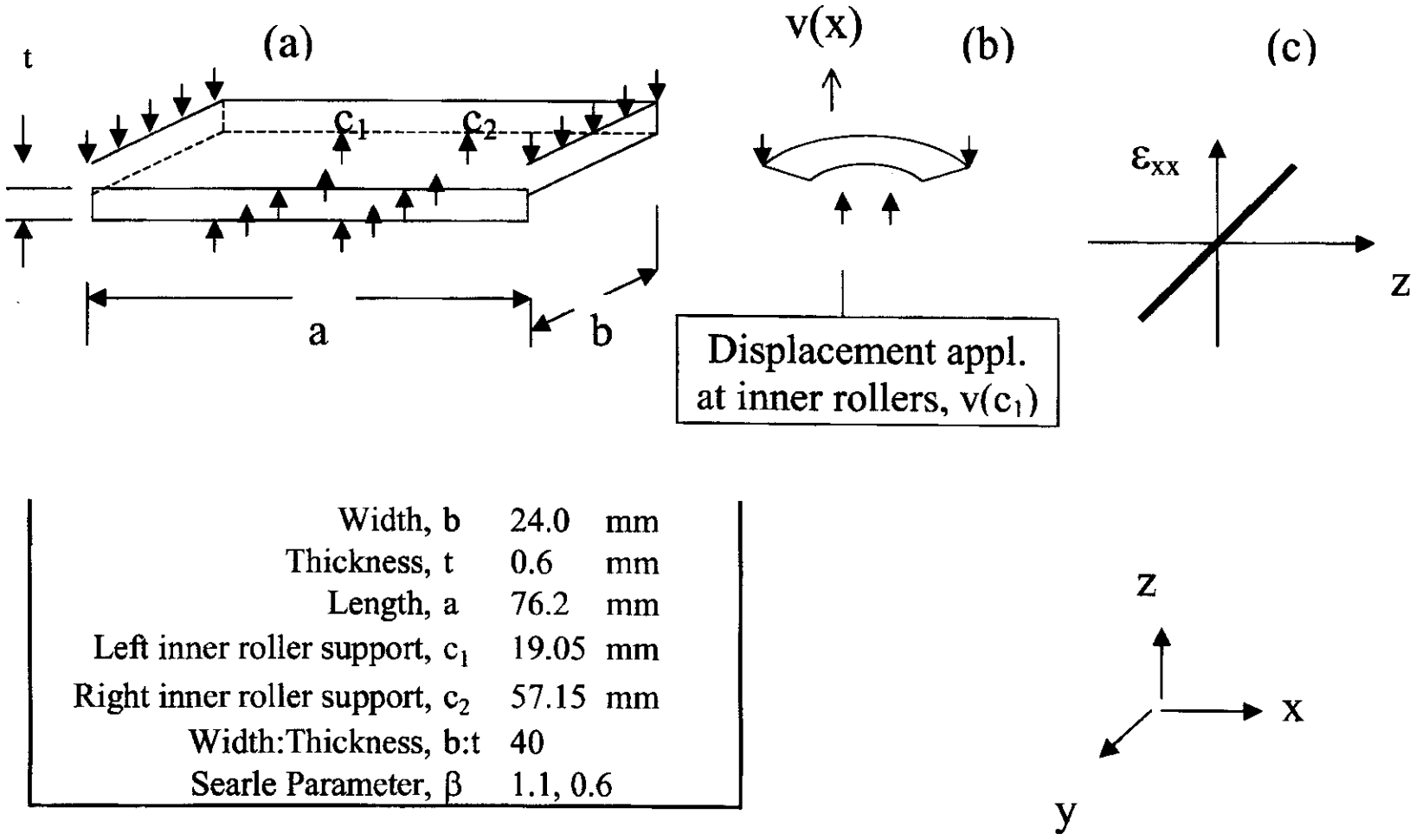

Width, b	24.0	mm
Thickness, t	0.6	mm
Length, a	76.2	mm
Left inner roller support, c_1	19.05	mm
Right inner roller support, c_2	57.15	mm
Width:Thickness, b:t	40	
Searle Parameter, β	1.1, 0.6	

Figure 1. (a) Si specimen geometry and dimensions, (b) 2-D schematic of bent sample (displacement applied at c_1 and c_2 rollers), and (c) bending strain variation, ε_{xx}, with sample thickness, z.

KALDOR FIG. 1

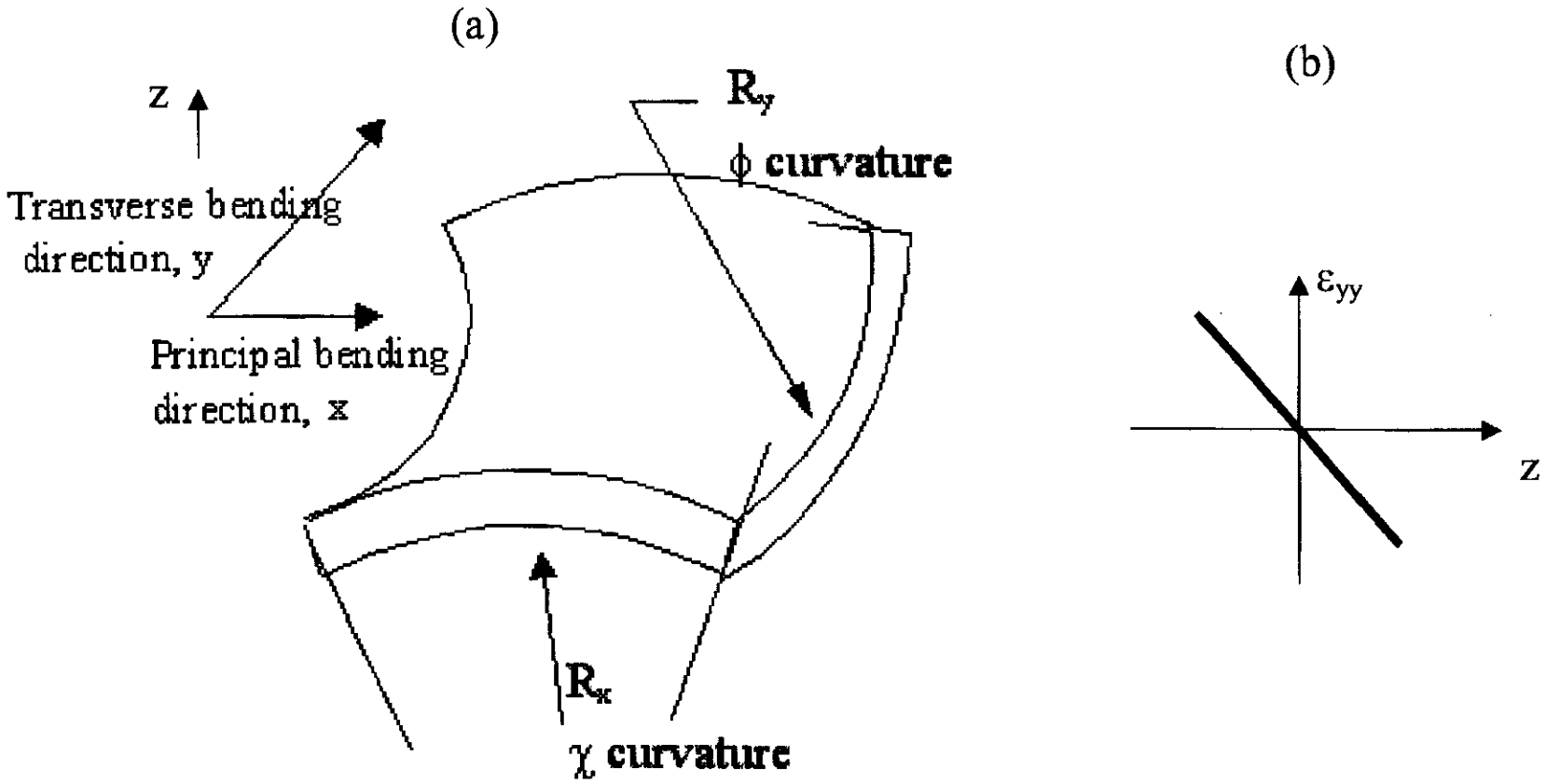

Figure 2. (a) The rectangular specimen is bent with a radius of curvature, R_x, along the principal bending direction, x. Poisson coupling causes the sample to bend along the transverse (y) direction with a radius of curvature, R_y, equal to R_x/ν thus resulting in an anticlastic, or saddle-shaped, surface. (b) The anticlastic-bending strain variation, ε_{yy}, with specimen thickness, z.

KALDOR FIG. 2

Figure 3. Schematic of the x-ray diffraction measurement. Given the correct Bragg angle (θ) between the sample surface and incident x-ray beam, x-rays will diffract from the Si (001) planes, i.e. those planes normal to the Si surface in a (100)-type crystal. For the unbent, flat single crystal in (a), the specimen tilt, ψ, necessary to satisfy the Bragg diffraction angle, θ, is independent of sample position. For the sample bent to a constant principal radius in (b), ψ necessary to satisfy θ will change with position along both the principal and transverse directions. The sample rotation required to satisfy the Bragg diffraction in (b) gives the specimen curvature.

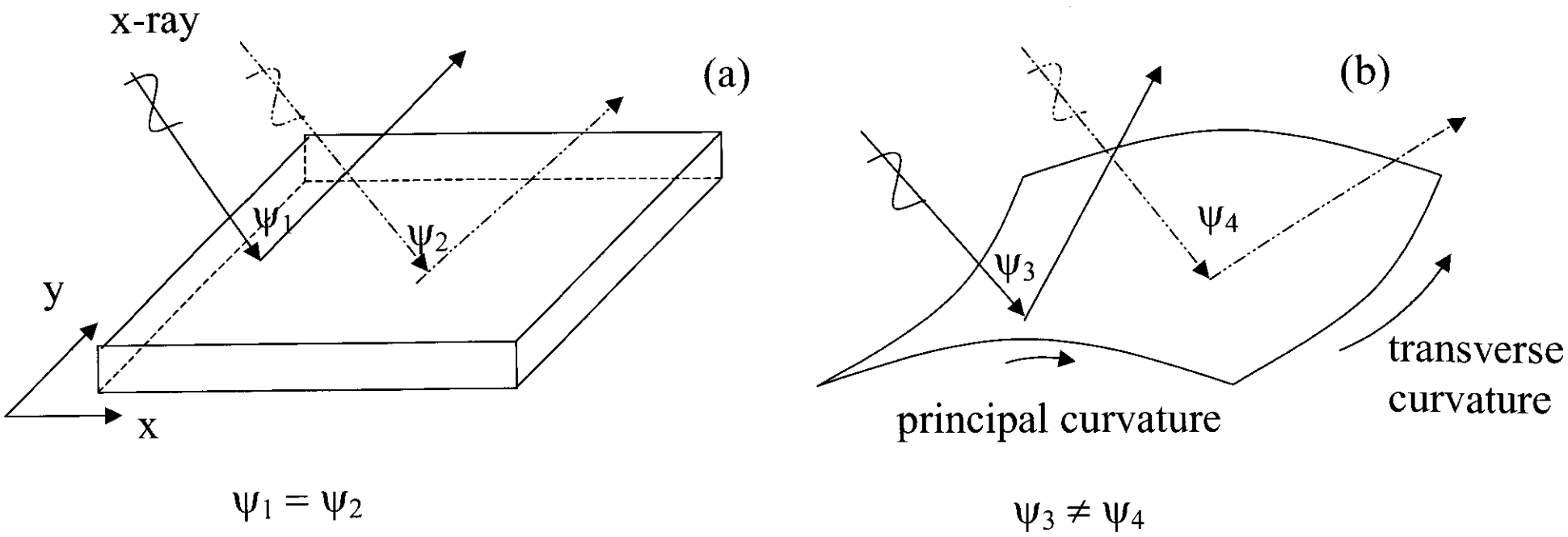

KALDOR FIG. 3

Figure 4. The sample tilt required to satisfy the Bragg condition for (004) diffraction from a Si (001) crystal as a function of position along the sample length at several distinct positions along the sample's width. The straight, overlapping lines indicate that the principal curvature constant between the two inner rollers and does not vary with position along the sample width. In (a) the principal bending axis is parallel to the <110> direction ($Si_{<001><110>}$) whereas in (b) it is parallel to the <100> ($Si_{<001><100>}$) direction.

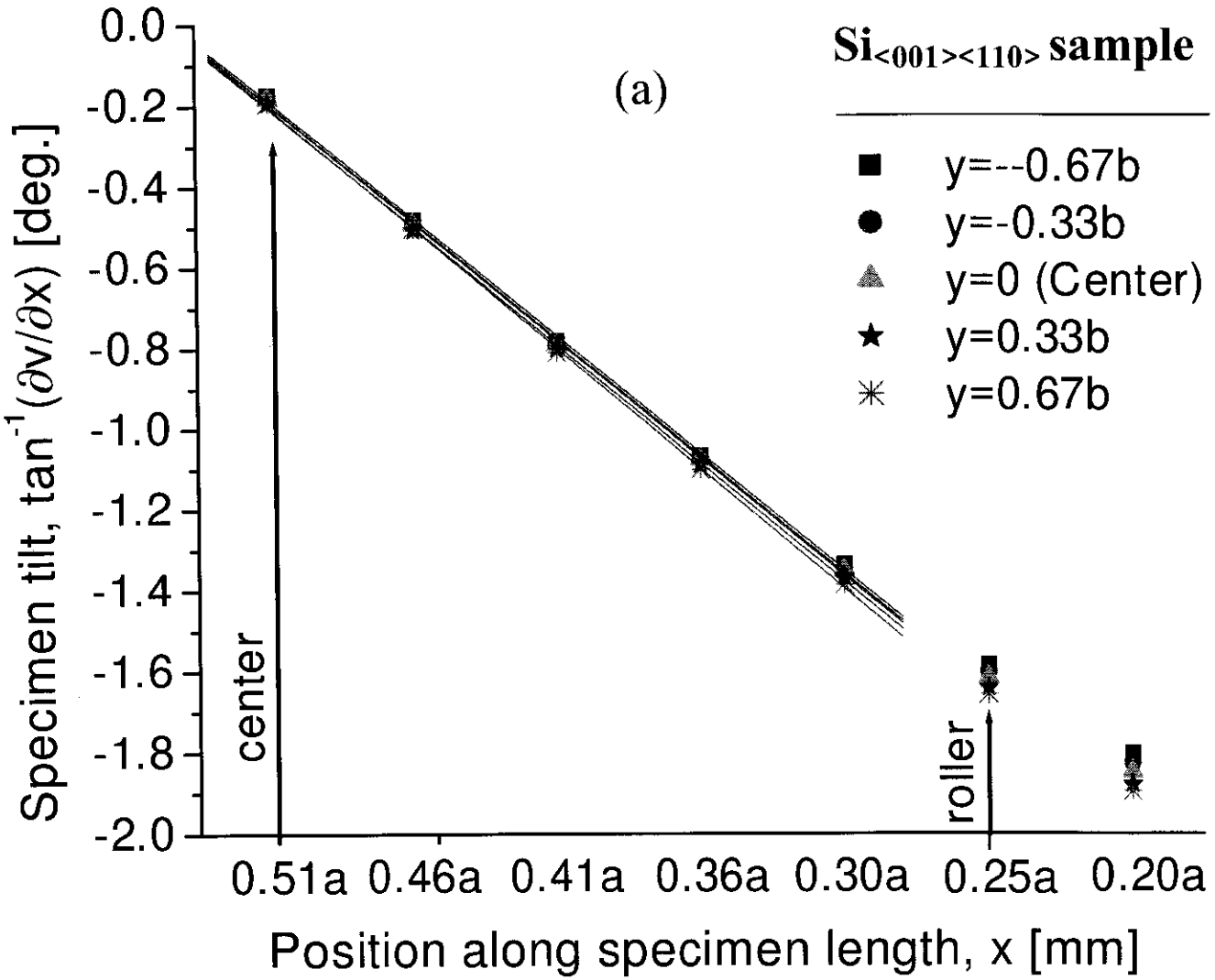

KALDOR FIG. 4a

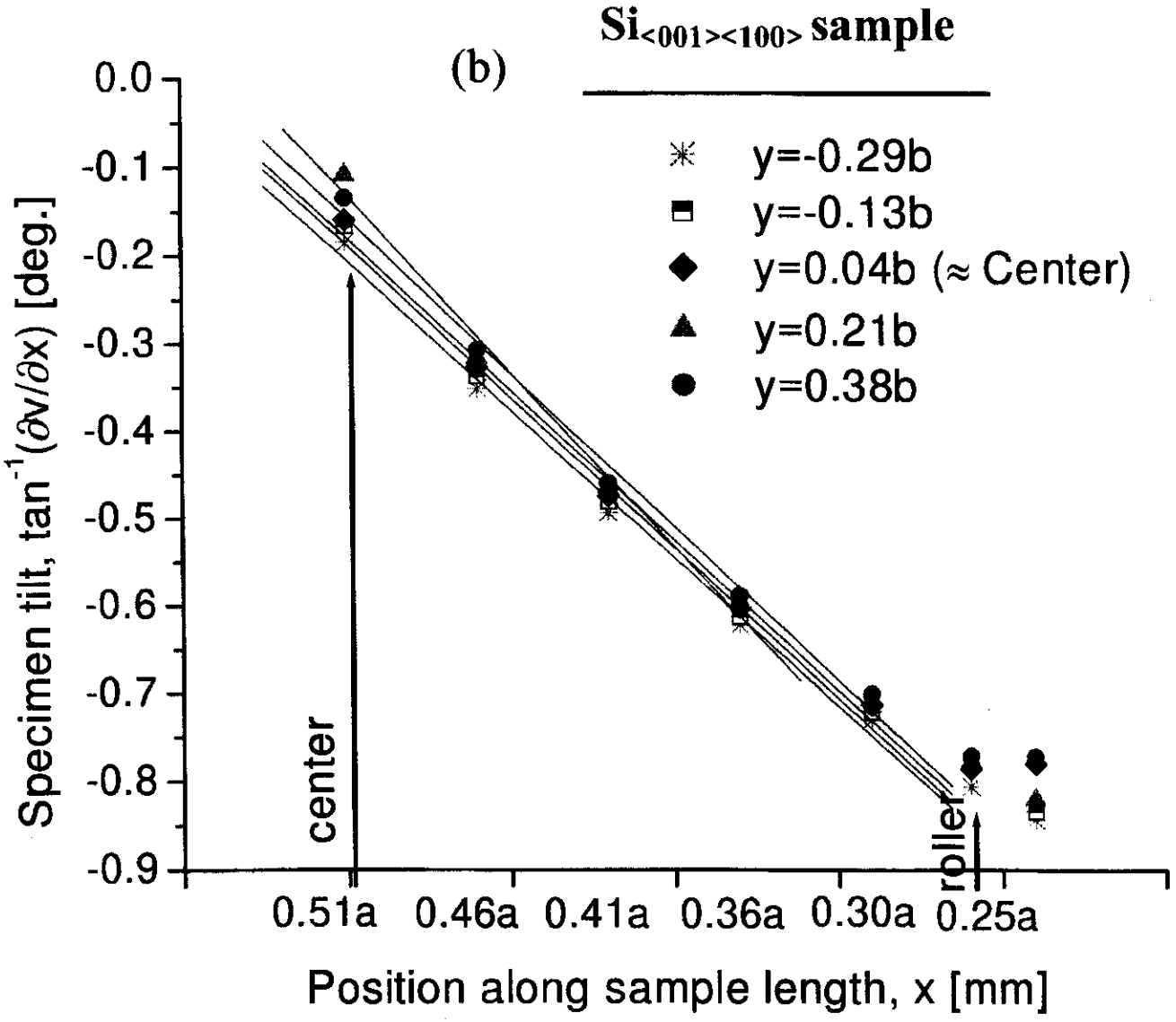

KALDOR FIG. 4b

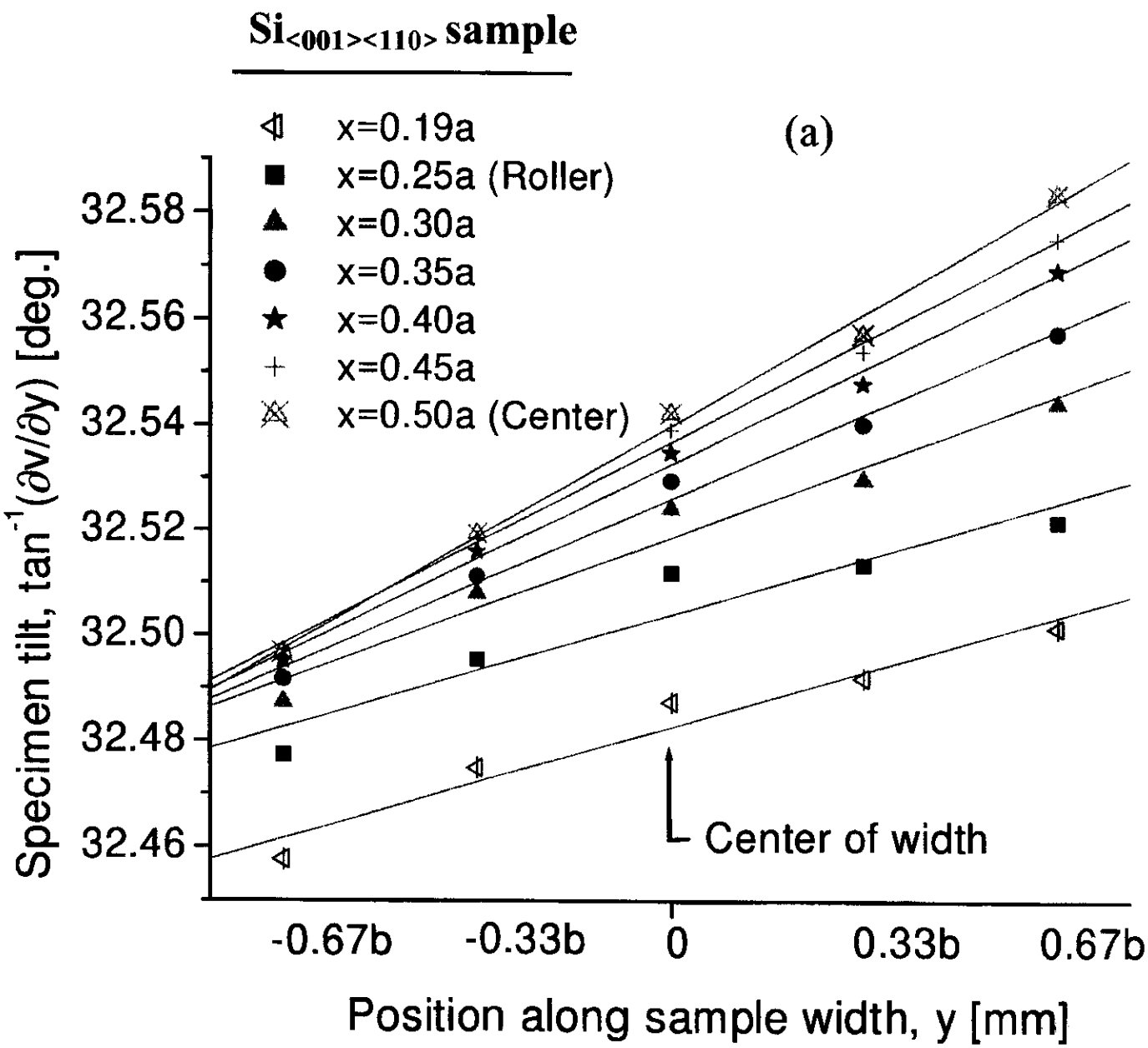

KALDOR FIG. 5a

Figure 5. The sample tilt required to satisfy the Bragg condition for (004) diffraction from a Si (001) crystal as a function of position along the sample width at several distinct positions along the sample's length. Unlike the principal curvature, these curves, whose slopes are a measure of anticlastic bending, vary with position along the sample length. In (a) the principal bending axis is parallel to the <110> direction ($Si_{<001><110>}$) whereas in (b) it is parallel to the <100> direction ($Si_{<001><100>}$).

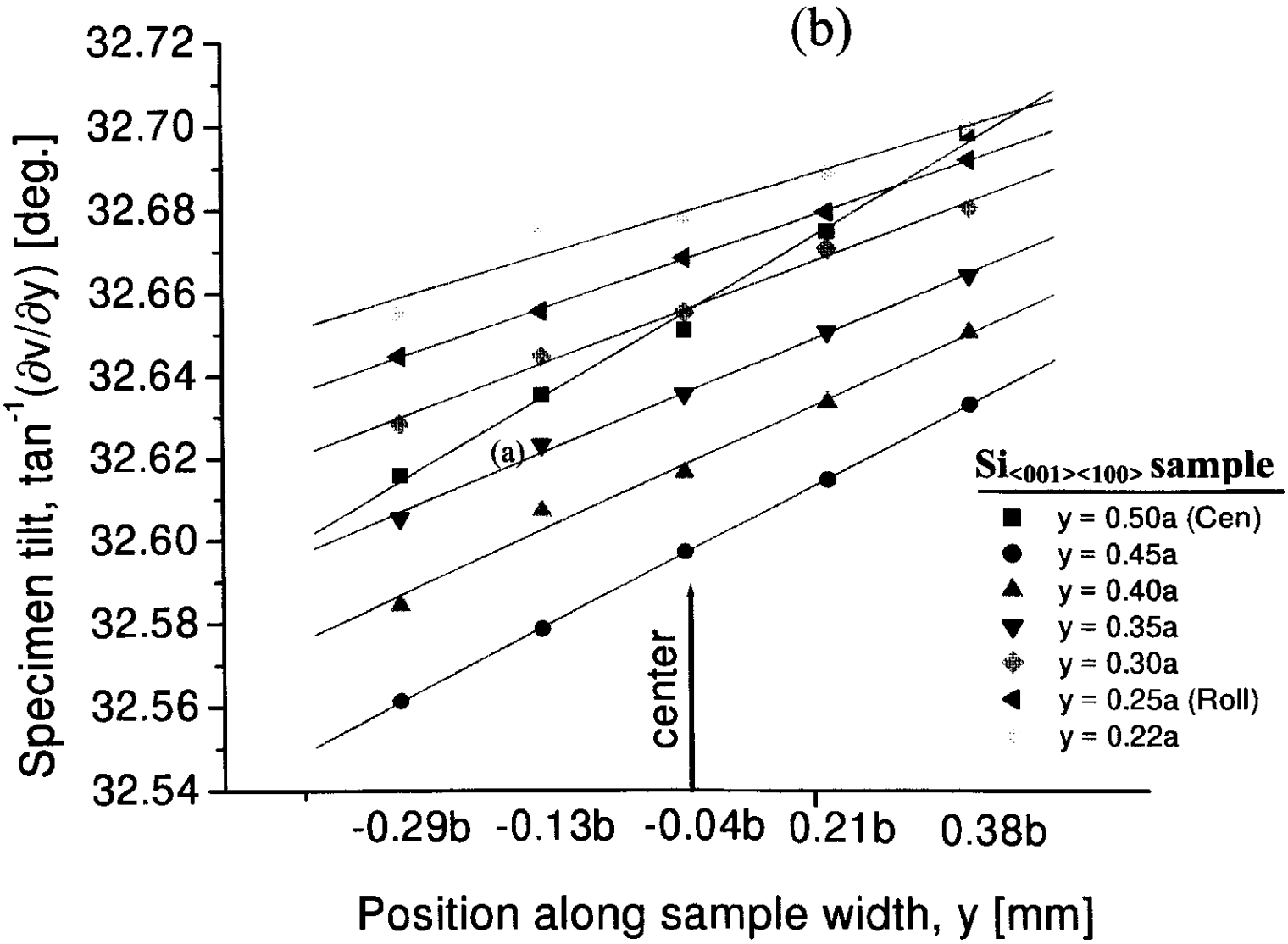

KALDOR FIG. 5b

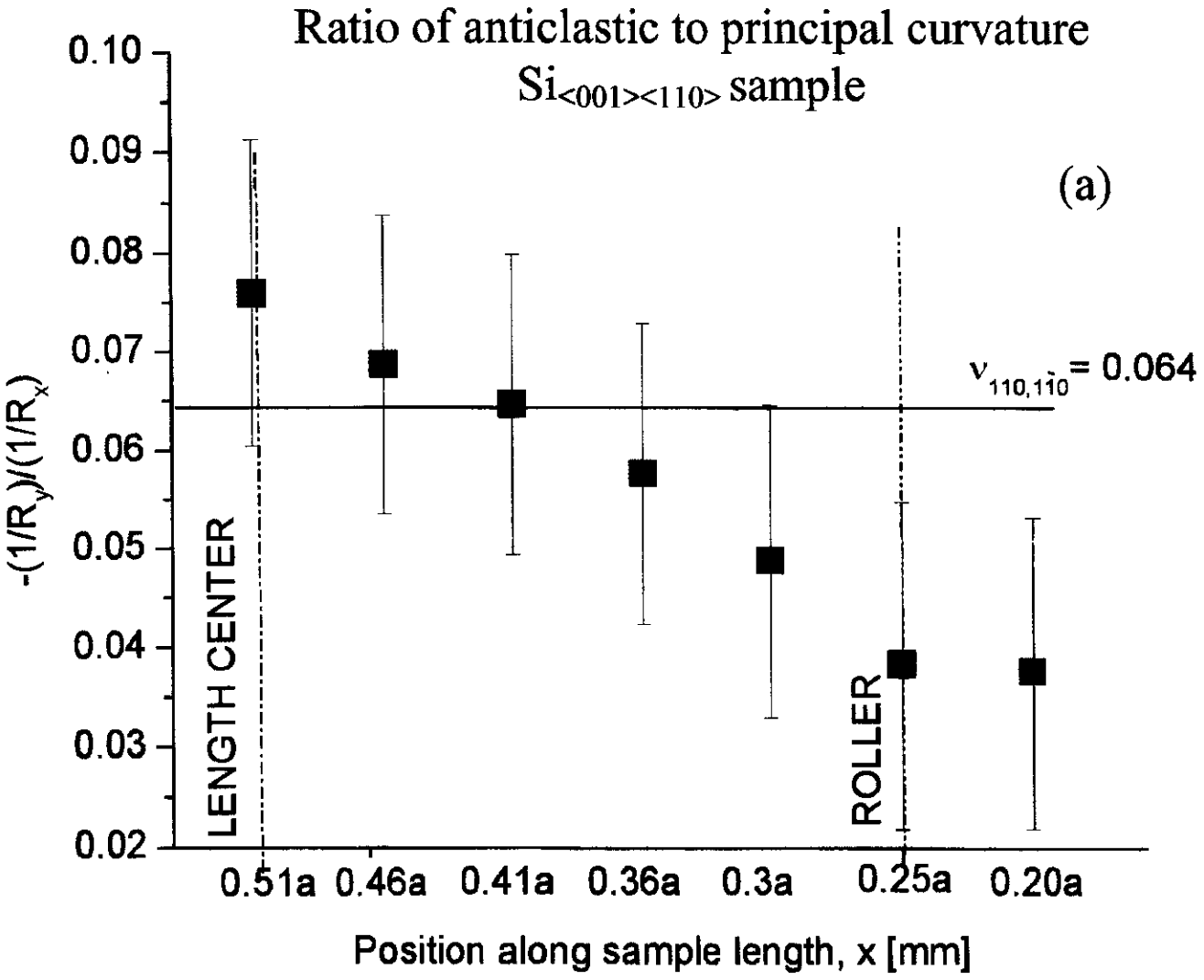

Figure 6. Variation of the ratio of transverse to principal curvatures with position along the sample length for (a) a $Si_{<001><110>}$ sample and (b) a $Si_{<001><100>}$ sample. The presence of rollers in this four-point loading configuration affects anticlastic bending.

KALDOR FIG. 6a

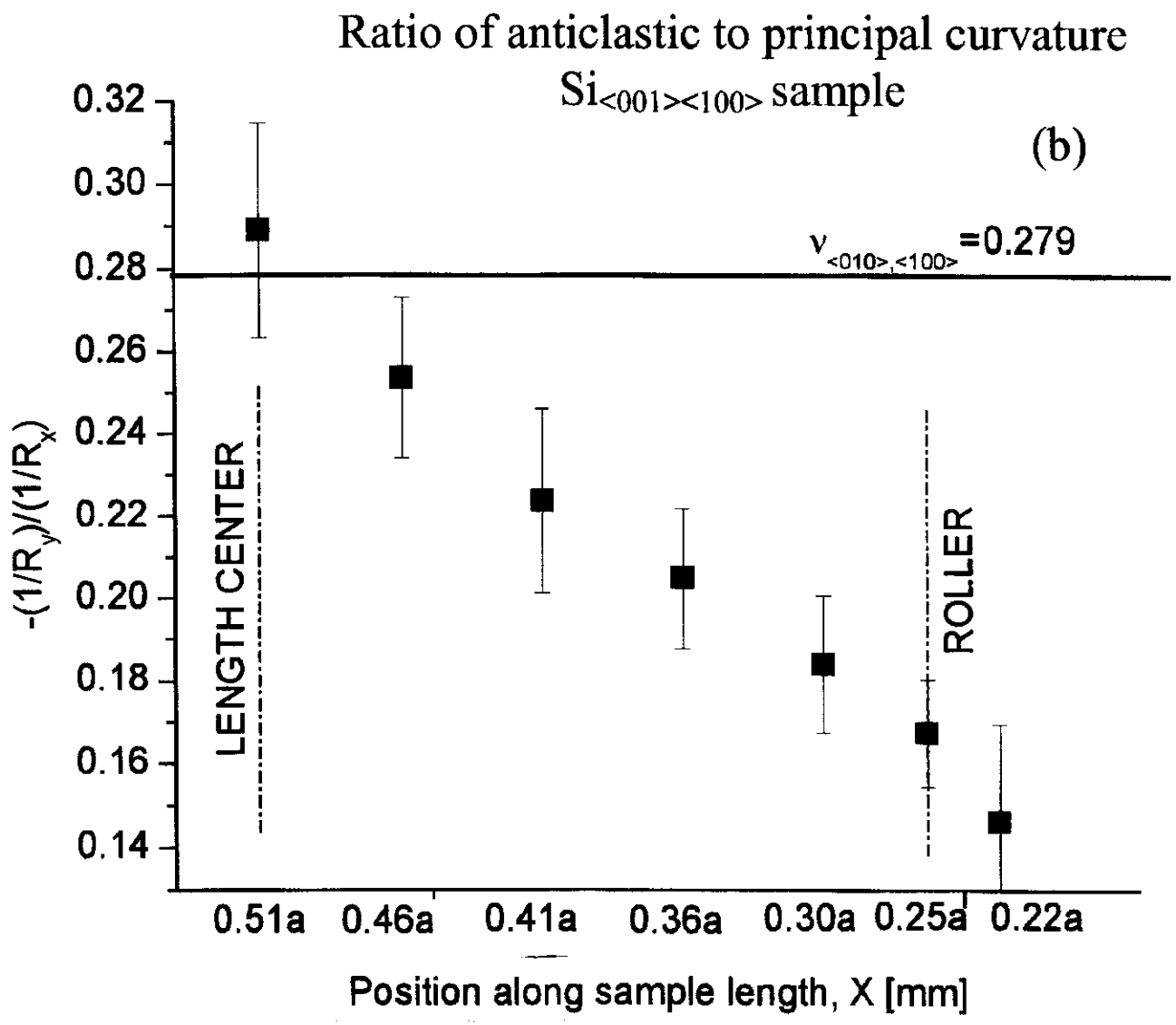

KALDOR FIG. 6b